The Retinoblastoma Protein and Its Homolog p130 Regulate the G_1/S Transition in Pancreatic β-Cells

George Harb,[1] Rupangi C. Vasavada,[1] David Cobrinik,[2] and Andrew F. Stewart[1]

OBJECTIVE—The retinoblastoma protein family (pRb, p130, p107) plays a central role in the regulation of cell cycle progression. Surprisingly, loss of pRb in the β-cell has no discernible effect on cell cycle control. Therefore, we explored the effects of individual loss of either p130 or p107 in addition to the simultaneous loss of both pRb/p130 on the β-cell.

RESEARCH DESIGN AND METHODS—Adult mice deficient in either p130 or p107 or both pRb/p130 were examined for effects on β-cell replication, function, and survival. The Cre-Lox system was also used to inactivate pRb in wild-type and p130-deficient β-cells in vitro.

RESULTS—In vivo loss of either p107 or p130 did not affect β-cell replication or function. Combined pRb/p130 loss, however, resulted in dramatically accelerated proliferation as well as apoptotic cell death. Pancreas and β-cell mass were significantly reduced in double mutants. Despite this, overall glucose tolerance was normal, except for mild postprandial hyperglycemia. Ex vivo, acute deletion of pRb in p130-deficient β-cells also caused a striking increase in proliferation. The combined deletion of pRb/p130 upregulated islet expression of E2F2 but not E2F1.

CONCLUSIONS—These studies define an essential role for the pocket proteins in controlling the G_1/S transition in β-cells. When deficient in both pRb and p130, β-cells undergo unrestrained cell cycle reentry and activation of apoptosis. These studies underscore the central role of the pRb pathway in controlling β-cell turnover and provide new cellular targets for β-cell regeneration.
***Diabetes* 58:1852–1862, 2009**

The pocket protein family consists of three members, the retinoblastoma tumor suppressor protein (pRb), p107, and p130. These proteins are believed to comprise the central regulatory checkpoint that controls the mammalian G_1/S-phase cell cycle transition. In the absence of pocket proteins, mouse embryonic fibroblasts are insensitive to G1 arrest signals and do not undergo senescence in culture (1,2). In the nonphosphorylated active state, pocket proteins interact with E2F transcription factors and inhibit E2F-responsive genes, which are required for cell cycle progression. This inhibition is relieved when cyclin-dependent kinases phosphorylate pocket proteins, altering their conformation, liberating E2Fs, and thereby permitting passage through the G_1/S checkpoint (3).

p130 and p107 were identified approximately a decade after pRb as homologous proteins that play critical roles in the regulation of cell proliferation (4–8). Common to all three pocket proteins is the ‘pocket’ domain that interacts with the E2Fs as well as with viral oncoproteins and the ability to induce growth arrest when overexpressed (1,5,9). In addition, all three can repress E2F-mediated gene transcription, recruit chromatin remodeling enzymes, and undergo phosphorylation by cyclin-dependent kinases (9,10). Despite these similarities, there exist extensive dissimilarities, both structural and functional, among the three members. For example, p130 and p107 transcriptionally regulate distinct classes of gene targets, enabling them to play distinct roles in the regulation of cell cycle progression (11). In addition, whereas pRb interacts predominantly with E2F1, E2F2, and E2F3, p130 and p107 interact primarily with E2F4 and E2F5 (9). Further, the associations between individual pocket proteins and their cognate E2F partners occur at distinct times throughout the cell cycle, reflecting, in part, differences in the temporal expression of each pocket protein throughout the cell cycle (9).

A role for pocket proteins in regulating the β-cell cycle was first suggested in 1985 by the observation that transgenic mice that express SV40 large T-antigen in the β-cell (RIP-TAg mice) develop hyperinsulinemia, hypoglycemia, and ultimately islet tumors (12). Large T-antigen binds to and inactivates pRb, p130, and p107 as well as other cellular proteins (13). However, it remains uncertain from these studies whether the increased β-cell replication in RIP-TAg mice resulted from inactivation of any one or multiple pocket proteins or effects on other proteins outside the pocket protein family.

The question as to which of the three pocket proteins is sufficient or necessary to restrict β-cell cycle progression has only recently begun to be investigated. We recently reported that β-cell–specific inactivation of the *Rb* gene alone has surprisingly little effect on β-cell replication, function, and survival (14). However, it is possible, and perhaps likely, that germline (i.e., chronic, life-long) inactivation of *Rb* in β-cells results in, or allows for, functional compensation by one or both of the other pRb-related members of the pocket protein family, p130 or p107. Interestingly, although both p130 and p107 are known to be present in murine pancreatic islets (15), their function has never been evaluated in the β-cell. To address this question, we assessed β-cell replication, function, and glucose homeostasis in both $p130^{-/-}$ and $p107^{-/-}$ mice. We also sought to address the possibility of functional

From the [1]Division of Endocrinology and Metabolism, Department of Medicine, University of Pittsburgh School of Medicine, Pittsburgh, Pennsylvania; and the [2]Margaret M. Dyson Vision Research Institute, Weill Medical College of Cornell University, New York, New York.
Corresponding author: Andrew F. Stewart, stewarta@pitt.edu.
Received 7 June 2008 and accepted 11 May 2009.
Published ahead of print at http://diabetes.diabetesjournals.org on 9 June 2009. DOI: 10.2337/db08-0759.
D.C. is currently affiliated with the Memorial Sloan-Kettering Cancer Center, New York, New York.
© 2009 by the American Diabetes Association. Readers may use this article as long as the work is properly cited, the use is educational and not for profit, and the work is not altered. See http://creativecommons.org/licenses/by-nc-nd/3.0/ for details.
The costs of publication of this article were defrayed in part by the payment of page charges. This article must therefore be hereby marked “advertisement” in accordance with 18 U.S.C. Section 1734 solely to indicate this fact.

compensation through the simultaneous genetic reduction of multiple pocket proteins (pRb and p130) in the β-cell. These studies reveal an essential and dramatic role for the pocket protein family in the control of the β-cell G_1/S transition.

RESEARCH DESIGN AND METHODS

Mouse models. Homozygous mutant mice with disrupted *p107* ($p107^{-/-}$) or *p130* ($p130^{-/-}$) genes were previously prepared and described by Cobrinik and Lee (16,17). Both mutant genes function as null alleles (16,17). For generation of *Rb/p130* double mutants, mice in which exon 19 of the *Rb1* gene is flanked by loxP recombination sites ($Rb^{lox/lox}$) (18) were crossed with $p130^{-/-}$ animals. The resultant $Rb^{lox/+};p130^{+/-}$ mice were intercrossed to generate $Rb^{lox/lox};p130^{-/-}$ mice. Concurrently, *RIP-Cre* transgenic mice (14,19) in which *Cre* expression is under the control of the rat insulin II promoter (14) were crossed with $p130^{-/-}$ mice to generate $RIP\text{-}Cre;p130^{-/-}$ animals. Crossing the compound mutants generated $Rb^{lox/+};p130^{-/-};Cre$ mice, which were backcrossed again to $Rb^{lox/lox};p130^{-/-}$ mice to produce a β-cell conditional knockout (CKO) of *Rb* in $p130^{-/-}$ mutant mice ($Rb^{lox/lox};p130^{-/-};Cre$ referred to as $Rb^{CKO};p130^{-/-}$). The breeding strategy is summarized in additional detail in the Figures. Mice that were either wild type for *Rb* ($Rb^{lox/lox}$ or $Rb^{lox/+}$; *Cre*-negative) or heterozygous ($Rb^{lox/+}$; *Cre*-positive) on a $p130^{-/-}$ background were also analyzed for comparison. All studies were performed on adult mice, 2- to 4-months of age, on a mixed C57/BL6–129 genetic background, with males and females being comparably represented. All studies were approved in advance by, and performed in compliance with, the University of Pittsburgh Institutional Animal Care and Use Committee.

Islet isolation and culture. Islets were isolated from adult mice as previously described (14,15). Briefly, islets were obtained from collagenase (Sigma, St. Louis, MO) digested pancreases after purification on a Histopaque (Sigma) gradient.

Cell cycle analysis. To analyze cell cycle progression, islets were dispersed into single cells with 0.05% trypsin-EDTA (Invitrogen, Carlsbad, CA), suspended in chilled 70% ethanol, and kept overnight at 4°C. Fixed cells were treated with 100 units/ml RNAase A (Sigma) in PBS and stained with 50 μg/ml propidium iodide (Sigma) at room temperature for 30 min (20). The cell cycle phase distribution of 10,000 cells was determined by flow cytometry using a BD LSR II flow cytometer (Becton Dickinson Biosciences, San Jose, CA). Analysis of data, including determination of gates, was performed using Modfit LT 3.0 software (Verity Software House, Topsham, ME) using gating shown in supplementary Figs. S1 and S4 (available in the online-only appendix at http://diabetes.diabetesjournals.org/cgi/content/full/db08-0759/DC1).

Immunoblotting and PCR. Islet protein extractions were prepared as previously described (14,15). Immunoblotting was performed using primary antibodies for pRb (Pharmingen, 554136), p107 (Santa Cruz, C-18), p130 (Santa Cruz, C-17), p21 (Santa Cruz, F-5), p53 (Biomeda, V1003), phospho-p53 (Ser15) (Cell Signaling, 9286), Cre (Convance, MMS-106P), E2F1 (Santa Cruz, C-20), and E2F2 (Santa Cruz, TFE-25) and secondary antisera as previously published (14,15). Mice were genotyped by PCR using previously described primers (14,16–18).

Glucose, insulin, and intraperitoneal glucose tolerance testing. Measurements of fasting and postprandial blood glucose and plasma insulin levels, as well as intraperitoneal glucose tolerance testing were performed as detailed previously (14,15).

β-cell mass, replication, and apoptosis. Six hours before being killed, mice were injected intraperitoneally with bromodeoxyuridine (BrdU; Sigma) (50 mg/kg body wt). Pancreata were fixed in Bouin's solution, embedded in paraffin, sectioned, and stained with insulin (Dako), BrdU (Abcam, Ab6326), Ki-67 (Neomarkers, SP6), or phosphohistone H3 (Millipore, 06-570) antibodies as previously described (14,15,20). For determination of β-cell death, pancreas sections were stained using the in situ cell death detection kit (Roche Diagnostics, Indianapolis, IN) for identification of transferase-mediated dUTP nick-end labeling (TUNEL) and insulin double-positive cells (20).

Adenoviral infection. Islets isolated from wild-type ($Rb^{+/+};p130^{+/+}$), $Rb^{lox/lox};p130^{+/+}$, and $Rb^{lox/lox};p130^{-/-}$ mice were dispersed into single cells with 0.05% trypsin-EDTA and transduced with a replication-deficient recombinant adenovirus that expresses green fluorescent protein (Ad.GFP) or *Cre* recombinase (Ad.Cre) (a gift from Dr. Chris Newgard). Cells were transduced at a multiplicity of infection of 200 for 2 h at 37°C, plated on coverslips, and studied 72 h later. BrdU (1:1,000, Amersham) was added for the final 24 h of culture. Whole islets were also transduced and cultured for 72 h then frozen for immublot or PCR analysis.

Statistical analysis. All data are presented as means ± SE. Comparisons of multiple means were performed using ANOVA with SPSS 16.0 statistical software (Chicago, IL). $P < 0.05$ was considered significant.

RESULTS

The pRb homologs *p130* and *p107* are dispensable for adult mouse β-cell function and mass. Mice with inactivating mutations in p130 or p107 have previously been developed and characterized (16,17). These mice develop normally, are fertile, and apart from modest skeletal changes in *p107* mutants, exhibit no obvious adult phenotypes. However, these previous studies did not include any assessment of β function or glucose homeostasis. The gene-targeting strategies used to disrupt the *p130* or *p107* genes (16,17) are shown in Fig. 1*A* and supplementary Fig. S1A (available in the online-only appendix). Mutant mice were identified by PCR analysis of genomic DNA and confirmed as nulls by immoblotting for p130 or p107 in isolated islets (Fig. 1*B*; supplementary Fig. S1*B*, available in the online-only appendix). Metabolic analysis of adult *p130*- or *p107*-deficient mice revealed a completely normal phenotype, similar to that seen in mice with *Rb*-null islets. Specifically, body weight, fasting and postprandial blood glucose, and plasma insulin values were entirely normal compared with heterozygous and wild-type littermates (Fig. 1*C–F*; supplementary Fig. S1*C–F*, available in the online-only appendix). Glucose tolerance was also normal in mice lacking *p130* or *p107*, compared with wild-type littermates (Fig. 1*D*; supplementary Fig. S1*D*, available in the online-only appendix).

Consistent with normal glucose tolerance in the mutants, pancreas and β-cell mass were also normal in both *p130*- and *p107*-null animals (Fig. 2*A*; supplementary Fig. *S*2A, available in the online-only appendix). Histomorphometric analysis of whole pancreas sections immunostained for insulin revealed that, as with pRb (14), p130 and p107 are also entirely dispensable for normal pancreas and β-cell growth (Fig. 2*B*; supplementary Fig. S2*B*, available in the online-only appendix).

In vivo loss of *p130* or *p107* does not affect β-cell cycle control. Like pRb, p130 and p107 also regulate cell cycle progression (9). Adult differentiated β-cells that have exited the cell cycle and entered a state of quiescence express both p130 and p107 (Fig. 3*B*) (14,20). Therefore, we speculated that loss of p130 or p107 in β-cells might result in aberrant cell cycle reentry. Instead, loss of either p130 or p107 failed to affect β-cell replication rates (Fig. 3*A*; supplementary Fig. S4*A*, available in the online-only appendix) and islet cell cycle phase distribution (supplementary Figs. S1 and S4*B*, available in the online-only appendix). This may result from functional compensation within the retinoblastoma family because there was a striking upregulation of p107 protein in p130-null islets (82.4 ± 4.0%) (Fig. 3*B*). These findings demonstrate that p130 and p107 are individually dispensable for maintaining β-cell cycle arrest in adult mouse β-cells.

pRb and *p130* cooperatively regulate the adult β-cell G_1/S transition in vivo. The preceding data suggest that in the absence of an individual pocket protein, functional redundancy among the remaining members may be sufficient to maintain cell cycle arrest in β-cells. Therefore, we generated mutant mice in which β-cells were deficient for both pRb as well as p130. Inactivation of both the *Rb* and *p130* genes was selected because disruption of both *p130* and *p107* is embryonic lethal (17) and because a previous

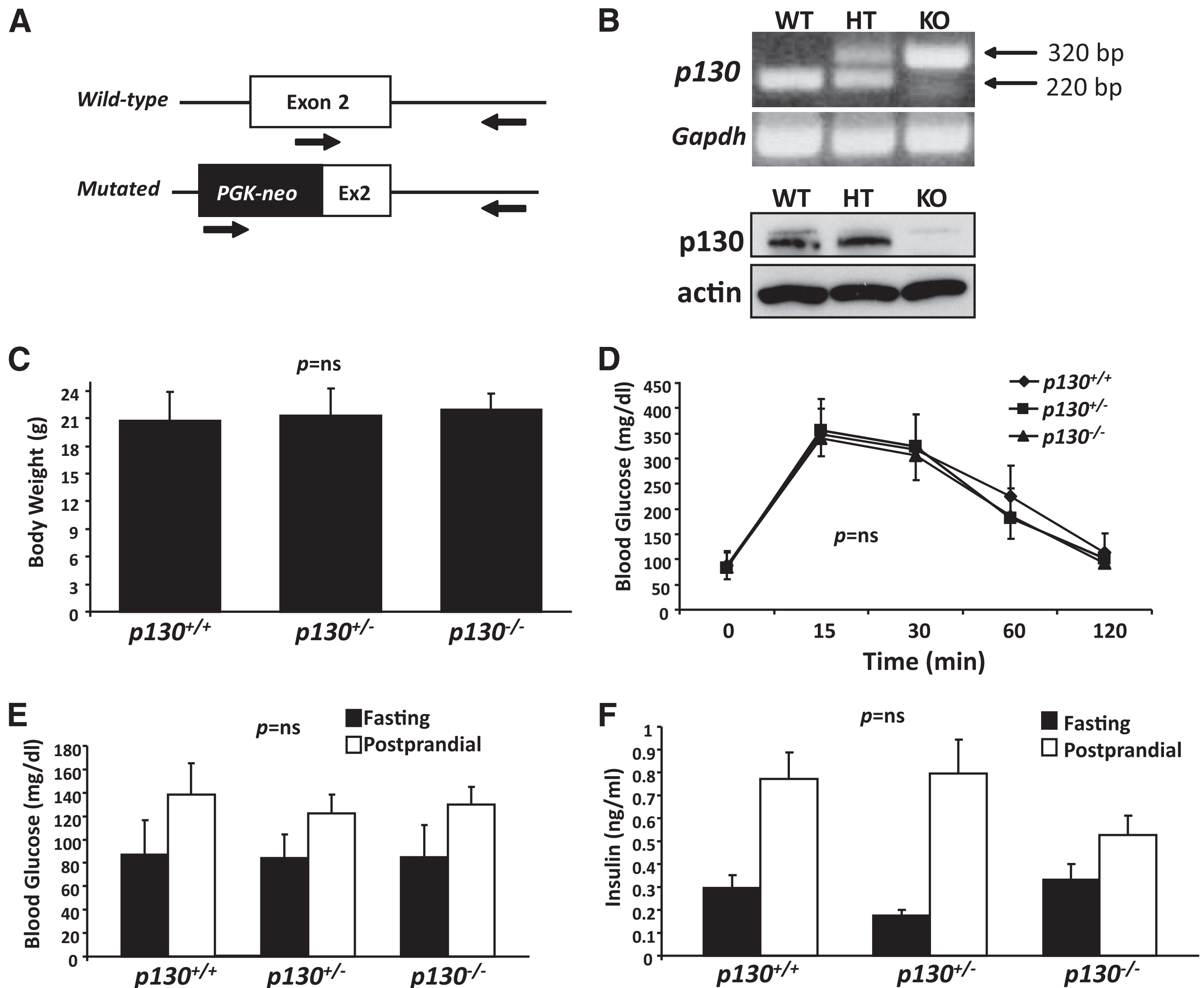

FIG. 1. Targeted disruption of the *p130* gene and metabolic characterization of *p130*-null mice. *A*: The *p130* gene was disrupted by insertion of a targeting vector into exon 2 (17). Mutant alleles that contain the neomycin resistance gene (neo) were detected using PCR with previously described primers represented by arrows (17). *B*: (*upper*) PCR products for genomic DNA from *p130* wild-type (WT), heterozygous (HT), and knockout (KO) animals. The mutant *p130* gene was identified based on amplification of a 320-bp PCR fragment. *Gapdh* was used as an internal control. *B*: (*lower*) A representative immunoblot of islet protein extracts from *p130* WT, HT, and KO animals probed with a p130 antibody. Actin was used to ensure equal protein loading in all immunoblots. *C–F*: Metabolic characterization of *p130*-null mice. At the time of a glucose tolerance test, fasted animals were weighed (*C*), then injected intraperitoneally with a glucose bolus. *D*: Shows the blood glucose levels of animals at the indicated time points following glucose administration. Blood obtained from fasting and postprandial mice were analyzed for circulating glucose (*E*) and insulin (*F*). There were no statistically significant differences between the KO (n = 6–8) and WT (n = 7–9) or HT (n = 7–9) mice. *PGK*, phosphoglycerate kinase; *neo*, neomycin.

study reported that one out of 15 $Rb^{+/-}p130^{-/-}$ mutant mice developed an insulinoma, an effect not observed in $Rb^{+/-}p107^{-/-}$ mutant mice (21). To disrupt both *Rb* and *p130* simultaneously, β-cell–specific pRb CKO (Rb^{CKO}) mice (Fig. 4*A*) (14) were crossed with *p130*-null mice to generate compound Rb^{CKO};$p130^{-/-}$ double-knockout mutant mice (Fig. 4*B*). In addition, mice that were wild type or heterozygous for *Rb* on a $p130^{-/-}$ background (Rb^{WT};$p130^{-/-}$ and Rb^{HT};$p130^{-/-}$, respectively) were also analyzed for comparison. PCR analysis of genomic DNA was used for identification of double-mutant animals based on the presence of floxed *Rb* alleles (283-bp), the *Cre* transgene, and the 320-bp mutant *p130* gene (Fig. 4*C*). Immunoblot analysis of pRb and p130 revealed only faint residual levels of pRb, likely reflecting expression of pRb in the few non–β-cells of isolated islets (fibroblasts, α-cells, endothelial cells, etc.) and absent p130 protein in extracts of isolated Rb^{CKO};$p130^{-/-}$ islets (Fig. 4*D*).

The percentage of replicating β-cells was determined by immunofluorescent staining of Rb^{WT};$p130^{-/-}$ and Rb^{CKO};$p130^{-/-}$ pancreatic sections for both insulin and Ki67. Loss of both pRb and p130 resulted in an 11-fold increase in the percentage of β-cells expressing Ki67 compared with control β-cells (3.2 ± 0.6% in Rb^{CKO};$p130^{-/-}$ vs. 0.3 ± 0.1 in Rb^{WT};$p130^{-/-}$, $P < 0.05$) (Fig. 5*A*). β-Cell entry into S phase (BrdU^{+}) also increased dramatically (14-fold) in the absence of both pRb and p130 (3.8 ± 0.7% in Rb^{CKO};$p130^{-/-}$ vs. 0.3 ± 0.1% in Rb^{WT};$p130^{-/-}$, P = 0.004) (Fig. 5*B*). Finally, there was a 30-fold increase in the number of

FIG. 2. Islet histomorphometry in *p130*-null mice. *A*: Representative insulin-stained sections of whole pancreata and quantification (*B*) of β-cell mass and area based on pancreas mass that were not significantly different in the three groups. WT (n = 9), HT (n = 5), and KO (n = 7). (A high-quality digital representation of this figure is available in the online issue.)

β-cells entering mitosis as assessed using phosphorylation of histone H3 (PHH3) on serine 10 (Fig. 5*C*).

To determine if increased β-cell death was associated with the accelerated cell division seen in *Rb*/*p130* double-mutant β-cells, we examined apoptotic β-cell death (Fig. 5*D*). In contrast to the very low number of apoptotic β-cells in control pancreata (0.05 ± 0.04%), β-cell death was strikingly increased in *Rb*/*p130*-deficient β-cells

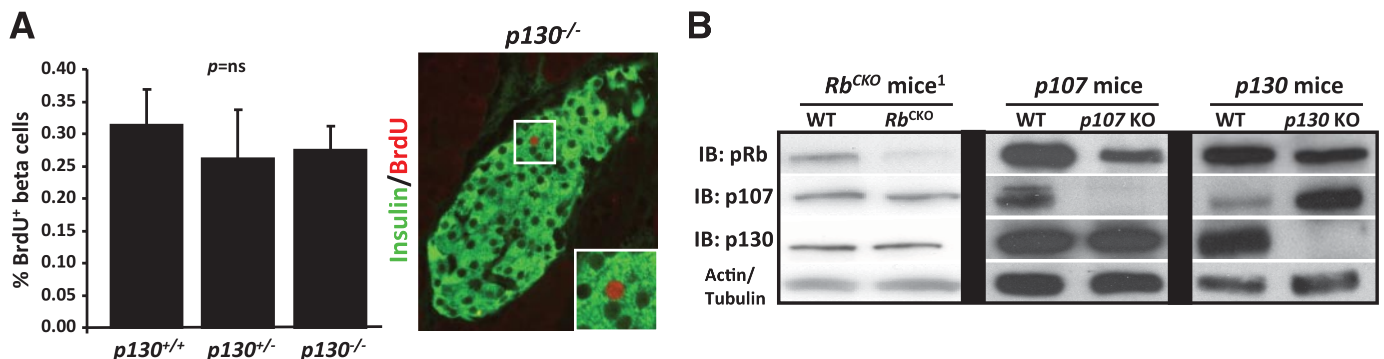

FIG. 3. β-cell replication in *p130*-null islets and compensatory upregulation of pocket protein family members. *A*: Quantification of β-cell replication (%$BrdU^+$-$insulin^+$ cells). Replication was not significantly increased in *p130*-deficient β-cells (n = 5) compared with WT (n = 9) or HT (n = 5) mice. *B*: Representative immunoblots of Rb^{CKO}, *p107*, or *p130* WT or KO islet protein extracts probed for pRb, p107, and p130. Note that the data for Rb^{CKO} mice have been previously published by Vasavada et al. (14) and are included for comparison of the data on p107 and p130. (A high-quality digital representation of this figure is available in the online issue.)

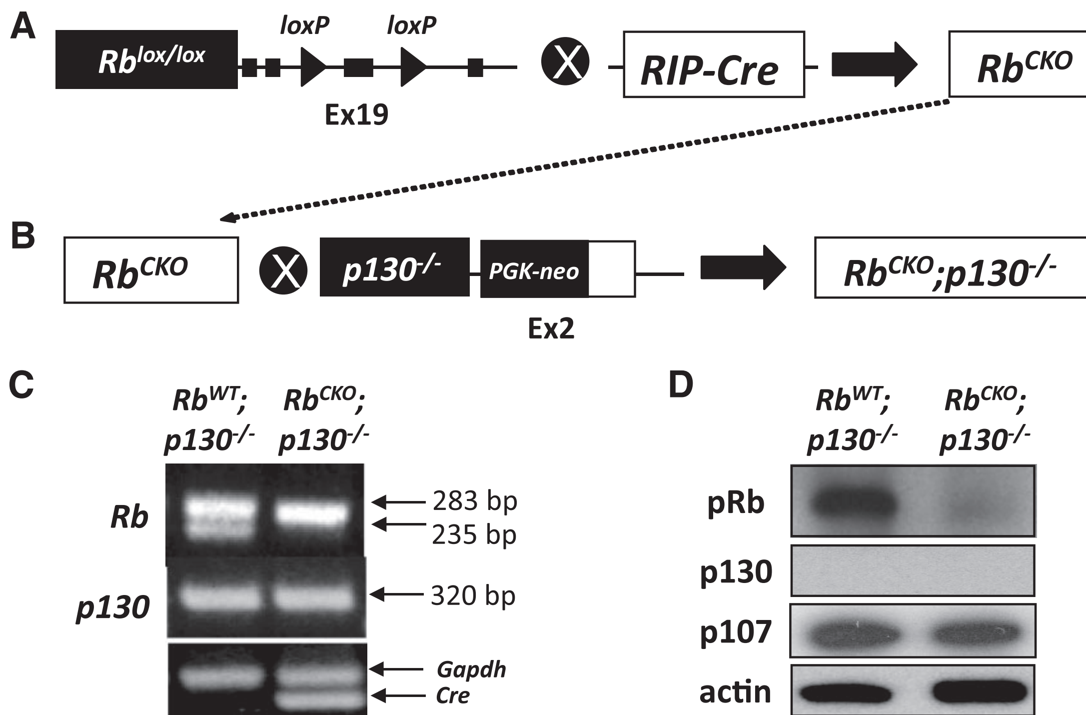

FIG. 4. Simultaneous inactivation of *Rb* and *p130* genes in double-mutant mice. *A*: Generation of β-cell–specific pRb conditional knockout mice (Rb^{CKO}) has been previously described by our group (14). Mice that contain *loxP* sequences surrounding exon 19 of the *RB* gene were crossed with *RIP-Cre* mice resulting in excision of the flanked region (18) *B*: The Rb^{CKO} mice were crossed with $p130^{-/-}$ mice to obtain $Rb^{CKO};p130^{-/-}$ double-mutant mice. *C*: PCR analysis of the *Rb* 283-bp product represents the floxed allele whereas the 235-bp allele represents the wild-type *Rb* gene. The 320-bp product represents mutant *p130*. The *lower panel* indicates uniform amplification of the *Gapdh* housekeeping standard and the *Cre* transgene. *D*: Immunoblot analysis of pRb and p130 protein in isolated pancreatic islets reveals deficiency of the two proteins in $Rb^{CKO};p130^{-/-}$ double-mutant animals.

(1.8 ± 0.2%, P = 0.001 vs. controls) (Fig. 5*D*). The mechanism underlying the increased β-cell apoptosis appears to involve a p53-dependent pathway because phosphorylation of p53 protein was increased in Rb^{CKO}; $p130^{-/-}$ β-cells, as was protein expression of the p53 target gene, $p21^{CIP1}$ (Fig. 5*E*).

Pancreas and β-cell mass are significantly reduced in $Rb^{CKO};p130^{-/-}$ mutant mice. In contrast to mice that lack pRB, p130, or p107 individually in their β-cells, adult double-mutant mice had significantly smaller pancreata than controls (P = 0.001; Fig. 6*B*). This almost 50% reduction in pancreas mass remained significant even when adjusted for the approximate 20% reduction in body weight (P < 0.05; Fig. 6*A* and *B*, Fig. 7*A*). However, exocrine cell proliferation (BrdU$^+$) was not altered in $Rb^{CKO};p130^{-/-}$ animals compared with controls (0.03 ± 0.05% vs. 0.04 ± 0.04%, n = 3, P = ns). In addition, there was no change in exocrine cell death (TUNEL$^+$) in Rb^{CKO}; $p130^{-/-}$ pancreata compared with control pancreata (0.01 ± 0.01% vs. 0.01 ± 0.02%, n = 3, P = ns). The reduction in pancreas mass was accompanied by a significant reduction in β-cell mass, even when adjusted for body mass (Fig. 6*C*; P = 0.04 vs. $Rb^{WT};p130^{-/-}$). However, the ratio of β-cell area to total pancreas area was not reduced in double mutants, suggesting a proportional reduction in both exocrine and endocrine pancreatic mass (Fig. 6*C*).

$Rb^{CKO};p130^{-/-}$ mutant mice are only mildly metabolically abnormal despite increased β-cell turnover. Intraperitoneal glucose tolerance tests revealed that double mutants respond to a glucose challenge as efficiently as controls (Fig. 7*B*). However, random sampling of postprandial blood glucose levels revealed $Rb^{CKO};p130^{-/-}$ mice were mildly hyperglycemic (P < 0.05) compared with controls, whereas fasting blood glucose levels were similar (Fig. 7*C*). The postprandial hyperglycemia occurred despite normal levels of circulating plasma insulin in $Rb^{CKO};p130^{-/-}$ mice (Fig. 7*D*). Thus, despite a statistically significant reduction in β-cell mass, the slightly dwarfed $Rb^{CKO};p130^{-/-}$ mice contained a body weight–adjusted β-cell mass and function that allows them to maintain near-normal glucose homeostasis largely in the normal range.

Ex vivo deletion of pRb in $p130^{-/-}$ β-cells also causes increased proliferation. Off-target expression of the RIP promoter in the CNS is well described and conceivably might account for an islet phenotype. Thus, to determine whether the increase in β-cell proliferation in the double-mutant mice resulted from direct (β-cell) or indirect (CNS) effects of *pRb/p130* loss, we disrupted the *Rb* gene ex vivo in both wild-type and $p130^{-/-}$ β-cells using the *Cre-LoxP* method of gene recombination. Isolated β-cells from $Rb^{lox/lox};p130^{+/+}$ or $Rb^{lox/lox};p130^{-/-}$ animals were transduced with an adenovirus expressing *Cre* recombinase (Ad.Cre). Expression of *Cre* in β-cell nuclei could be detected within 24 h after infection (Fig. 8*A*). This resulted in efficient deletion of exon 19 at 72 h after transduction (Fig. 8*B*). Cre-mediated deletion of pRb resulted in a reduction in pRb protein levels, associated with an increase in both p130 and p107 in $Rb^{lox/lox};p130^{+/+}$ islets (Fig. 8*C*). $Rb^{lox/lox};p130^{-/-}$ islets displayed upregulated p107 expression. This was further increased after deletion of pRb. Loss of both pRb and p130 resulted in elevated E2F2, but not E2F1, as assessed by immunoblot.

Most importantly, in agreement with the results obtained from *pRb/p130* mutant mice in vivo, disruption of both pRb and *p130* in β-cells ex vivo also caused a striking

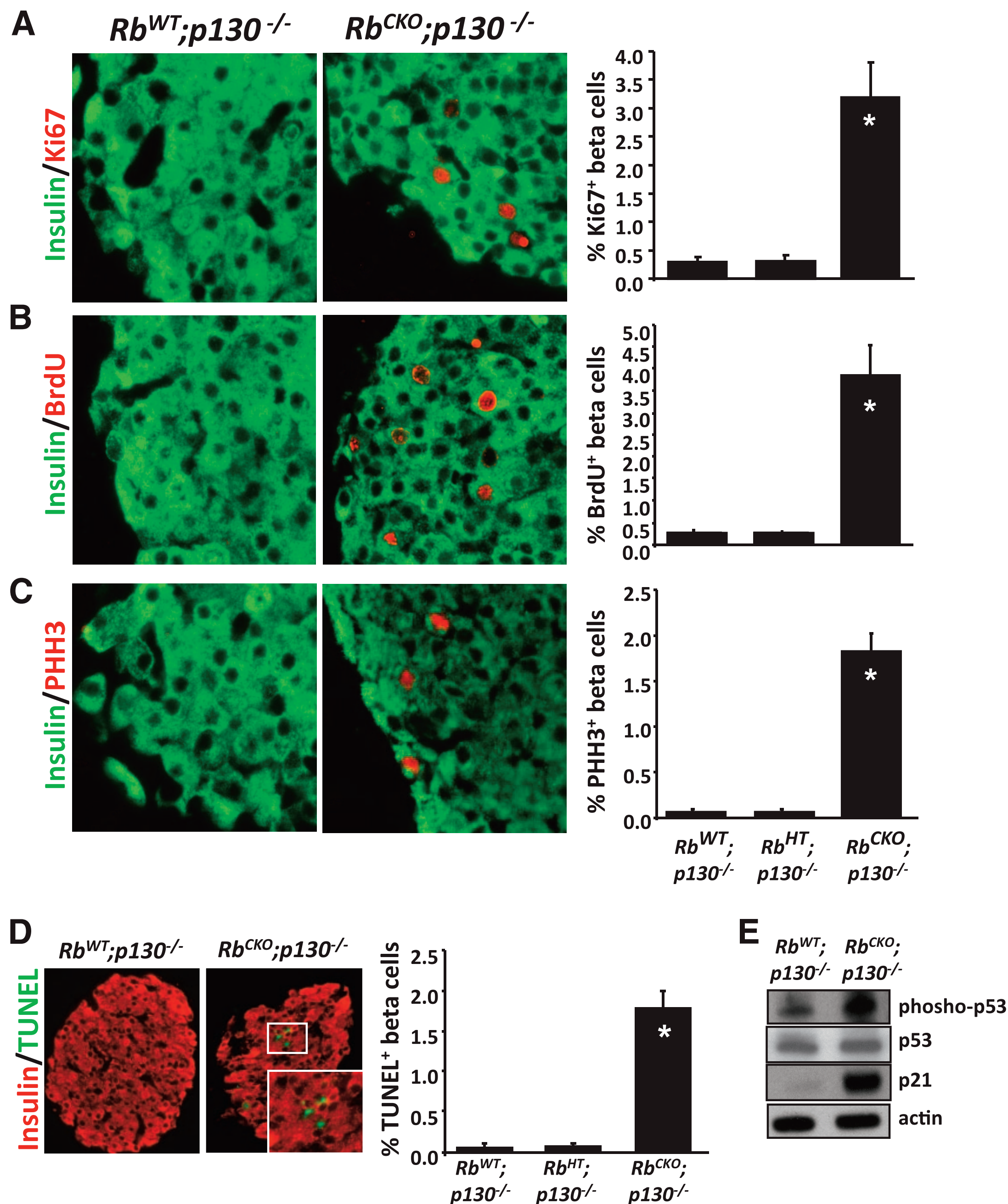

FIG. 5. Cell cycle progression and apoptosis in *Rb/p130* double-deficient β-cells. Pancreatic sections from $Rb^{WT};p130^{-/-}$ and $Rb^{CKO};p130^{-/-}$ animals are shown fluorescently stained for insulin (green) and (*A*) Ki67 (red), (*B*) BrdU (red), or (*C*) PHH3 (red). Quantitative analysis of the percentage of double-positive β-cells is in the right column for each proliferative marker (*A–C*). $Rb^{WT};p130^{-/-}$ ($n = 5$), $Rb^{HT};p130^{-/-}$ ($n = 4$), $Rb^{CKO};p130^{-/-}$ ($n = 5$). *$P < 0.05$ compared with $Rb^{WT};p130^{-/-}$ and $Rb^{HT};p130^{-/-}$ (×400 magnification) *D*: β-cell apoptosis detection in $Rb^{WT};p130^{-/-}$, $Rb^{HT};p130^{-/-}$, and $Rb^{CKO};p130^{-/-}$ pancreata by insulin-TUNEL colabeling and quantification. *$P < 0.05$ compared with $Rb^{WT};p130^{-/-}$ and $Rb^{HT};p130^{-/-}$. *E*: Representative immunoblots for phospho-p53, p53, and p21 in islets from $Rb^{WT};p130^{-/-}$ or $Rb^{CKO};p130^{-/-}$ animals. Each blot was performed 3–5 times. (A high-quality digital representation of this figure is available in the online issue.)

19-fold increase in BrdU-incorporation (31.1 ± 5.2% Ad.Cre vs. 1.6 ± 1.3% Ad.GFP, $P < 0.05$) (Fig. 8*D* and *E*). Ad.Cre transduction of wild-type or $Rb^{+/+};p130^{-/-}$ islets had no effect on replication (Fig. 8*D* and *E*).

DISCUSSION

This study demonstrates that individual inactivation of the pRb homologs, *p130* or *p107*, like pRb itself (14), is insufficient to cause abnormal β-cell cycle progression or impair the function of these cells in vivo. In contrast, we observe that simultaneous loss of two pocket proteins (pRb and p130) in the pancreatic β-cell results in strikingly increased rates of β-cell replication. This cell cycle acceleration is also accompanied by increased apoptosis in β-cells. Genetic disruption of multiple genes encoding cell cycle regulators in mice has demonstrated key roles for several proteins upstream of the pRb family (22,23). The final common pathway for enforcing cell cycle arrest has traditionally been believed to be pRb. Thus, it was surprising to learn that disruption of the *Rb* gene in the pancreatic β-cell is not sufficient to cause cell cycle progression (14). Based on these unanticipated findings, we sought to

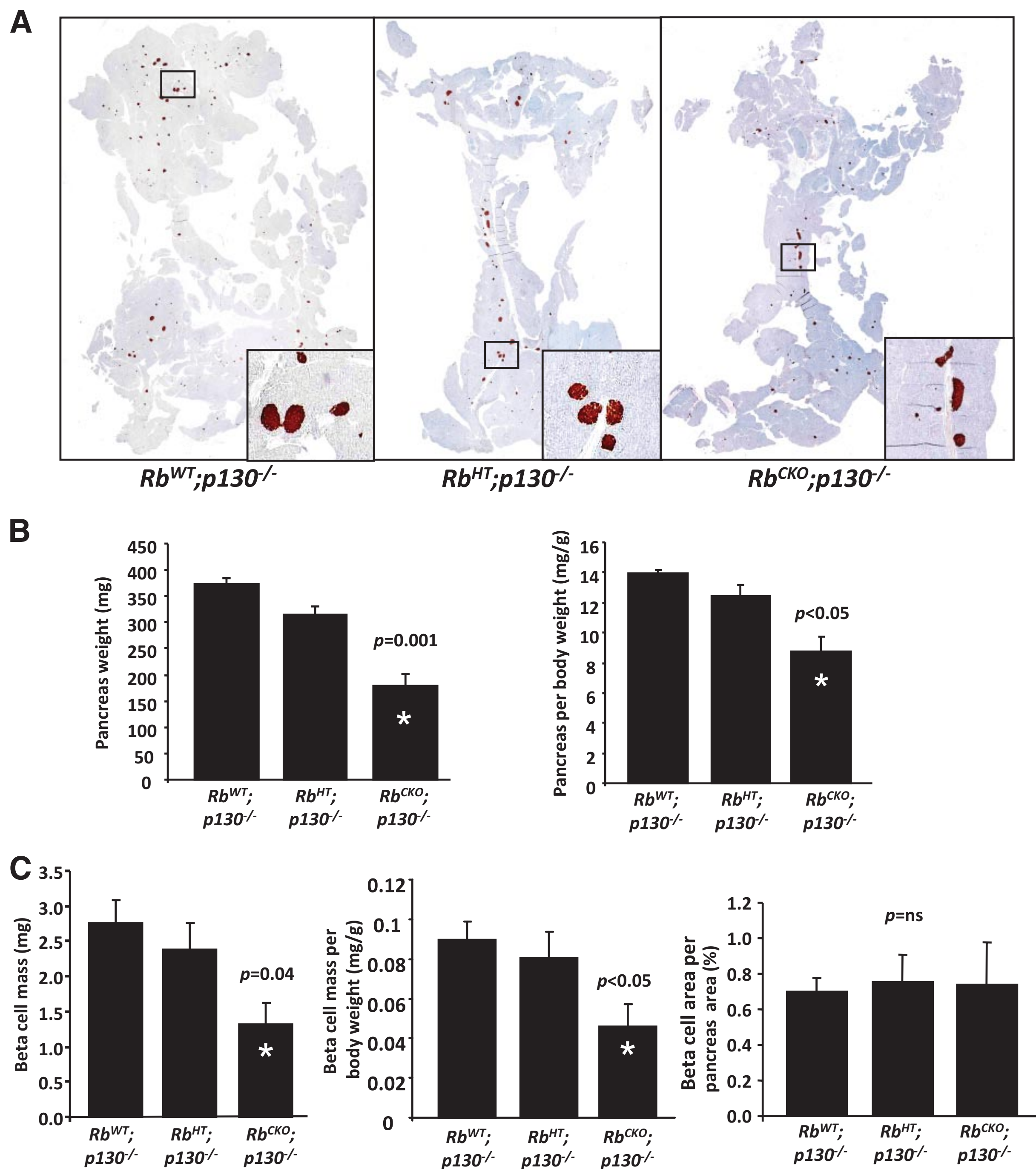

FIG. 6. Islet histomorphometry in *Rb/p130* double-mutant mice. *A*: Representative insulin-stained sections of whole pancreata from $Rb^{WT};p130^{-/-}$ (n = 9), $Rb^{HT};p130^{-/-}$ (n = 5), and $Rb^{CKO};p130^{-/-}$ (n = 9) animals. *B*: Shows quantification of pancreas mass as well as the pancreas-to-body weight ratio that were significantly reduced in $Rb^{CKO};p130^{-/-}$ mice (*P < 0.05). *C*: Shows a significant reduction in β-cell mass, also when adjusted for body weight (*P = 0.04 vs. $Rb^{WT};p130^{-/-}$). β-cell area per pancreas area was similar in all three groups. (A high-quality digital representation of this figure is available in the online issue.)

examine whether the two remaining pocket proteins, p130 or p107, might play a regulatory role in β-cell proliferation. Interestingly, like mice with pRb-null islets, adult $p130^{-/-}$ or $p107^{-/-}$ mice also displayed normal glucose homeostasis as well as quantitative β-cell histomorphometry and replication rates. From these studies, it appeared that individual pocket proteins are entirely dispensable for maintaining β-cell cycle arrest, or that the individual loss of pRb, p130, or p107 is functionally compensated by another pocket protein family member. These findings are consistent with broad compensation among the pocket protein family members (3,9,10).

Studies on mice lacking individual pocket proteins may fail to highlight the significance of any one particular family member because of complementary and overlapping roles. Perhaps the best example of this is the *Rb*-null mouse that does not develop retinoblastoma unless either *p130* or *p107* are also removed (21). In this study, we found an upregulation of p107 protein in *p130*-null islets (Fig. 3*B* and 8*C*), which has also been observed in other

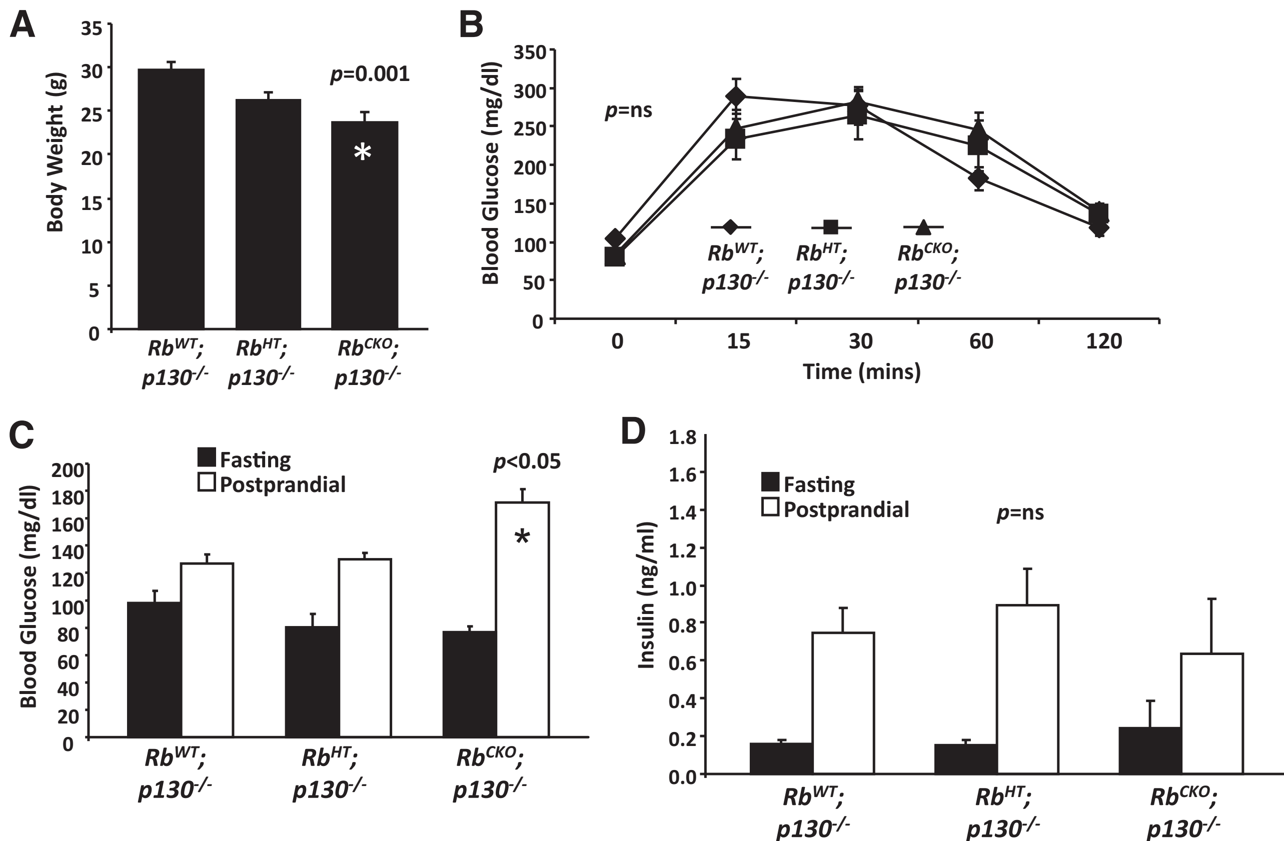

FIG. 7. Metabolic characterization of *Rb/p130* double-mutant mice. At the time of a glucose tolerance test, fasted animals were weighed (*A*), then injected intraperitoneally with a glucose bolus. *B*: Shows the blood glucose levels of animals at the indicated time points after glucose administration. Blood from fasting and postprandial mice was analyzed for circulating glucose (*C*) and insulin (*D*). Body weight is significantly reduced in Rb^{CKO};$p130^{-/-}$ animals (n = 9) compared with Rb^{WT};$p130^{-/-}$ (*P = 0.001; n = 9) but not Rb^{HT};$p130^{-/-}$ mice (n = 5). Random postprandial glucose is significantly elevated (*P < 0.05) in Rb^{CKO};$p130^{-/-}$ animals compared with control mice.

Rb- (1,24) or *p130*-null (21,25) cell types. Increased levels of p107 have also been demonstrated to be responsible for enforcing cell cycle arrest in *Rb*-null MEFs because down-regulation of p107 expression by siRNA molecules resulted in increased proliferation (24). Therefore, we speculated that in our model of unperturbed normal β-cell growth, individual or single loss of pRb, p130, or p107 may be compensated for by the redundant antiproliferative effects of the other two pocket proteins. Interestingly, in islets from $p107^{-/-}$ mice, neither pRb or p130 levels were upregulated. Instead, we observed reduced levels of pRb in isolated $p107^{-/-}$ islets that has also been observed in $p107^{-/-}$ adult adipocyte precursors (26). The authors of that report implicated a role for the differing levels of pRb and p107 in preadipocyte differentiation. However, what role these proteins play in β-cell differentiation from their progenitors is unknown and warrants further investigation.

Several lines of evidence have suggested that overlapping functional roles for pocket proteins can be revealed when mice combinatorially lack multiple pocket protein members (25–29). Double-mutant mice with tissue-specific *Rb/p130* or *Rb/p107* inactivation have helped uncover redundancy among family members in specific cell types such as keratinocytes (27), cardiac myocytes (28), intestinal epithelial cells (29), and others. In fact, some tissues display more aggressive phenotypes depending on which combination of pocket proteins is inactivated. For example, intestinal epithelial cells revealed a significantly more robust phenotype in *Rb/p130* deficient animals than in *Rb/p107* double-mutant animals (29). Further, studies from doubly deficient *Rb/p130* and *Rb/p107* mice revealed that the tumor spectrum in these mice does not entirely overlap (21). This is apparently true for the pancreatic β-cell as well because insulinomas arose only in $Rb^{+/-}p130^{-/-}$ but not $Rb^{+/-}p107^{-/-}$ mice (21). Indeed, we found significantly elevated levels of β-cell replication were present in adult mice when both *Rb* and *p130* genes were fully inactivated.

Increases in cell cycle progression were observed using three different markers of replication (BrdU, Ki67, PHH3). Further, mutant β-cells were also capable of progressing into the late G2–early mitotic phase of the cell cycle as assessed using PHH3. The increase in β-cell proliferation was accompanied by parallel increases in the rate of cell death. This increase in cell death appeared to reflect activation of the p53 pathway because active phospho-p53 was elevated and because p21, downstream of p53, was also elevated. In agreement with these results, combined inactivation of *p53* and *Rb* ($p53^{+/-}Rb^{+/-}$ and $p53^{-/-}Rb^{+/-}$) was found to be sufficient for the development of insulinomas (30,31). The widespread apoptosis detected in *pRb/p130*-deficient β-cells has not been observed in other cell types deficient in pRb and p130 such as the myocardium (28) or intestinal epithelium (29). Whether loss of both pRb and p107 in the β-cell would similarly increase both cell cycle entry and apoptosis is in need of investigation. Studying β-cells deficient in all three pocket proteins will be required to reveal the collective role played by these proteins in regulating β-cell cycle

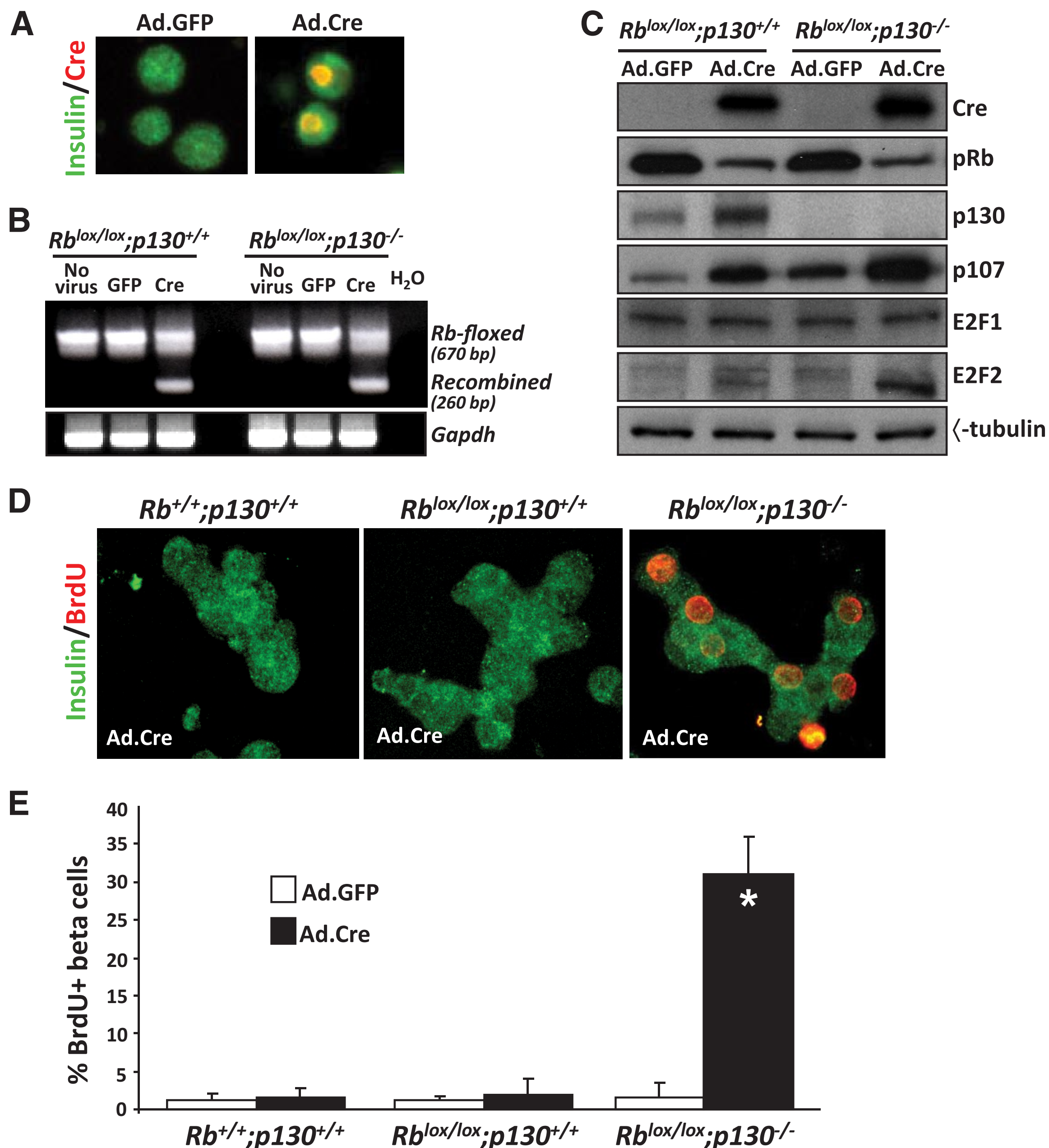

FIG. 8. Acute in vitro deletion of *Rb* in wild-type or *p130*$^{-/-}$ β-cells. *A*: Immunofluorescent detection of Cre (red) expression in the nuclei of β-cells stained for insulin (green) 24 h after transduction with Ad.Cre. *B*: PCR detection of Cre-mediated recombination of the *Rb* gene in *Rb*$^{lox/lox}$;*p130*$^{+/+}$ or *Rb*$^{lox/lox}$;*p130*$^{-/-}$ islets. PCR analysis of the floxed (670-bp) and recombined (260-bp) *Rb* alleles was performed 72 h after Ad.Cre transduction. The primers used to detect *Rb* and *Gapdh* alleles were previously reported by Vasavada et al. (14). *C*: Representative immunoblots for *Cre* recombinase, the pocket protein family, E2F1 and E2F2 from Ad.GFP, or Ad.Cre-transduced *Rb*$^{lox/lox}$;*p130*$^{+/+}$ or *Rb*$^{lox/lox}$;*p130*$^{-/-}$ islets (n = 3–4). *D*: Immunofluorescent staining of insulin (green) and BrdU (red) in *Rb*$^{+/+}$;*p130*$^{+/+}$, *Rb*$^{lox/lox}$;*p130*$^{+/+}$, or *Rb*$^{lox/lox}$;*p130*$^{-/-}$ β-cells transduced with either Ad.GFP or Ad.Cre followed by 72 h of culture (×400 magnification). *E*: Quantification of BrdU incorporation into *Rb*$^{+/+}$;*p130*$^{+/+}$ (n = 6), *Rb*$^{lox/lox}$;*p130*$^{+/+}$ (n = 7), or *Rb*$^{lox/lox}$;*p130*$^{-/-}$ (n = 6) β-cells transduced with either Ad.GFP (white bars) or Ad.Cre (black bars). *P < 0.05 versus Ad.GFP transduced β-cells from both groups. (A high-quality digital representation of this figure is available in the online issue.)

progression. Unfortunately, simultaneous loss of both *p130* and *p107* in mice results in neonatal lethality (17), so inactivation of all three members will require the generation of a triple–conditionally null mouse.

Pancreatic histology in the double-mutant mice, both endocrine and exocrine, was interesting. In the endocrine compartment, the β-cell mass was reduced as compared with body weight, presumably reflecting a mismatch in the rates of β-cell replication and cell death. In the exocrine compartment, total pancreas weight was also decreased (Fig. 6*B*), and this was disproportionate to the decline in body weight (Fig. 7*A*). The reasons for the decline in body weight and pancreatic weight are unclear, but both contrasted to liver, spleen, and kidney weights, which were comparable in all three groups of animals (supplementary Fig. S4, available in the online-only appendix). Pancreatic acinar cell proliferation and apoptosis rates were normal. We speculate that the decline in body weight may have resulted from development of pituitary or hypothalamic tumors, which are known to occur with pRb loss (32). This may well have occurred in our double-mutant mice, which were globally deficient for *p130* and may have been

pituitary/hypothalamic deficient for pRb as a result of "leaky" expression of RIP-Cre (14,33,34).

These considerations raise the possibility that the marked increases in β-cell replication and cell death might also have resulted from CNS misexpression of RIP-Cre. Thus, we performed ex vivo studies in isolated islets using adenoviral delivery of *Cre* recombinase (24). These studies revealed that combined pRb and p130 loss directly in β-cells led to markedly increased β-cell replication. In agreement with our previously published report on in vivo pRb deletion in β-cells (14), we again observed no increase in proliferation after in vitro deletion of pRb alone. However, unlike the in vivo studies, we did observe a compensatory increase in both p130 and p107 levels after acute pRb ablation. On the other hand, when pRb was reduced in β-cells already deficient for p130, we observed a dramatic increase in β-cell proliferation. The increased proliferation was associated with elevated E2F2 but not E2F1 levels. E2F2 is a member of the transcriptional activator E2Fs and has been shown, along with E2F1, to play an essential role in postnatal pancreas development (35,36).

In conclusion, this study demonstrates that both *Rb* and *p130* in combination are essential for normal pancreatic β-cell cycle control. Elucidation of therapeutic approaches that permit the stimulation of β-cell replication without induction of apoptosis may provide an approach to expand β-cells for the treatment of diabetes.

ACKNOWLEDGMENTS

G.H. is supported by a Juvenile Diabetes Research Foundation Fellowship Award (3–2008–35). A.F.S. is supported by National Institutes of Health Grant R-01 DK-55023.

No potential conflicts of interest relevant to this article were reported.

We thank the Don and Arleen Wagner and the Pam and Scott Kroh family foundations. We also thank Taylor Rosa and Karen Selk for assistance with the insulin radioimmunoassay and Adolfo Garcia-Ocaña and Irene Cozar-Castellano for their insightful critiques during the preparation of these studies. Finally, we thank Anton Berns for providing the $Rb^{lox/lox}$ mice.

REFERENCES

1. Sage J, Mulligan GJ, Attardi LD, Miller A, Chen S, Williams B, Theodorou E, Jacks T. Targeted disruption of the three Rb-related genes leads to loss of G(1) control and immortalization. Genes Dev 2000;14:3037–3050
2. Dannenberg JH, van Rossum A, Schuijff L, te Riele H. Ablation of the retinoblastoma gene family deregulates G(1) control causing immortalization and increased cell turnover under growth-restricting conditions. Genes Dev 2000;14:3051–3064
3. Cobrinik D. Pocket proteins and cell cycle control. Oncogene 2005;24: 2796–2809
4. Ewen ME, Xing YG, Lawrence JB, Livingston DM. Molecular cloning, chromosomal mapping, and expression of the cDNA for *p107*, a retinoblastoma gene product-related protein. Cell 1991;66:1155–1164
5. Zhu L, van den Heuvel S, Helin K, Fattaey A, Ewen M, Livingston D, Dyson N, Harlow E. Inhibition of cell proliferation by *p107*, a relative of the retinoblastoma protein. GenesDev 1993;7:1111–1125
6. Hannon GJ, Demetrick D, Beach D. Isolation of the Rb-related *p130* through its interaction with CDK2 and cyclins. Genes Dev 1993;7:2378–2391
7. Li Y, Graham C, Lacy S, Duncan AM, Whyte P. The adenovirus E1A-associated 130-kD protein is encoded by a member of the retinoblastoma gene family and physically interacts with cyclins A and E. Genes Dev 1993;7:2366–2377
8. Mayol X, Graña X, Baldi A, Sang N, Hu Q, Giordano A. Cloning of a new member of the retinoblastoma gene family (pRb2) which binds to the E1A transforming domain. Oncogene 1993;8:2561–2566
9. Classon M, Dyson N. *p107* and *p130*: versatile proteins with interesting pockets. Exp Cell Res 2001;264:135–147
10. Giacinti C, Giordano A. RB and cell cycle progression. Oncogene 2006;25: 5220–5227
11. Balciunaite E, Spektor A, Lents NH, H Cam H, Te Riele H, Scime A, Rudnicki MA, Young R, Dynlacht BD. Pocket protein complexes are recruited to distinct targets in quiescent and proliferating cells. Mol Cell Biol 2005;25:8166–8178
12. Hanahan D. Heritable formation of pancreatic β-cell tumours in transgenic mice expressing recombinant insulin/simian virus 40 oncogenes. Nature 1985;315:115–122
13. Zalvide J, DeCaprio JA. Role of pRb-related proteins in simian virus 40 large-T-antigen mediated transformation. Mol Cell Biol 1995;15:5800–5810
14. Vasavada RC, Cozar-Castellano I, Sipula D, Stewart AF. Tissue-specific deletion of the retinoblastoma protein in the pancreatic β cell has limited effects on β-cell replication, mass, and function. Diabetes 2007;56:57–54
15. Cozar-Castellano I, Weinstock M, Haught M, Velázquez-Garcia S, Sipula D, Stewart AF. Evaluation of β-cell replication in mice transgenic for hepatocyte growth factor and placental lactogen: comprehensive characterization of the G1/S regulatory proteins reveals unique involvement of *p21*cip. Diabetes 2006;55:70–77
16. Lee MH, Williams BO, Mulligan G, Mukai S, Bronson RT, Dyson N, Harlow E, Jacks T. Targeted disruption of *p107*: functional overlap between *p107* and Rb. Genes Dev 1996;10:1621–1632
17. Cobrinik D, Lee MH, Hannon G, Mulligan G, Bronson RT, Dyson N, Harlow E, Beach D, Weinberg RA, Jacks T. Shared role of the pRB-related *p130* and *p107* proteins in limb development. Genes Dev 1996;10:1633–1644
18. Marino S, Vooijs M, van Der Gulden H, Jonkers J, Berns A. Induction of medulloblastomas in *p53*-null mutant mice by somatic inactivation of Rb in the external granular layer cells of the cerebellum. Genes Dev 2000;14: 994–1004
19. Postic C, Shiota M, Niswender KD, Jetton TL, Chen Y, Moates JM, Shelton KD, Lindner J, Cherrington AD, Magnuson MA. Dual roles for glucokinase in glucose homeostasis as determined by liver and pancreatic β cell-specific gene knock-outs using *Cre* recombinase. J Biol Chem 1999;274:305–315
20. Cozar-Castellano I, Harb G, Selk K, Takane K, Vasavada R, Sicari B, Law B, Zhang P, Scott DK, Fiaschi-Taesch N, Stewart AF. Lessons from the first comprehensive molecular characterization of cell cycle control in rodent insulinoma cell lines. Diabetes 2008;57:1–13
21. Dannenberg JH, Schuijff L, Dekker M, van der Valk M, te Riele H. Tissue-specific tumor suppressor activity of retinoblastoma gene homologs *p107* and *p130*. Genes Dev 2004;18:2952–2962
22. Cozar-Castellano I, Fiaschi-Taesch N, Bigatel TA, Takane KK, Garcia-Ocaña A, Vasavada R, Stewart AF. Molecular control of cell cycle progression in the pancreatic β-cell. Endocr Rev 2006;27:356–370
23. Heit JJ, Karnik SK, Kim SK. Intrinsic regulators of pancreatic β-cell proliferation. Annu Rev Cell Dev Biol 2006;22:311–338
24. Sage J, Miller AL, Pérez-Mancera PA, Wysocki JM, Jacks T. Acute mutation of retinoblastoma gene function is sufficient for cell cycle re-entry. Nature 2003;424:223–228
25. Mulligan GJ, Wong J, Jacks T. *p130* is dispensable in peripheral T lymphocytes: evidence for functional compensation by *p107* and pRB. Mol Cell Biol 1998;18:206–220
26. Scimè A, Grenier G, Huh MS, Gillespie MA, Bevilacqua L, Harper ME, Rudnicki MA. http://www.ncbi.nlm.nih.gov/pubmed/16271529?ordinalpos=1&itool=EntrezSystem2.PEntrez.Pubmed.Pubmed_ResultsPanel.Pubmed_RVDocSumRb and *p107* regulate preadipocyte differentiation into white versus brown fat through repression of PGC-1alpha. Cell Metab 2005;2:283–295
27. Ruiz S, Santos M, Segrelles C, Leis H, Jorcano JL, Berns A, Paramio JM, Vooijs M. Unique and overlapping functions of pRb and *p107* in the control of proliferation and differentiation in epidermis. Development 2004;131: 2737–2748
28. MacLellan WR, Garcia A, Oh H, Frenkel P, Jordan MC, Roos KP, Schneider MD. Overlapping roles of pocket proteins in the myocardium are unmasked by germ line deletion of *p130* plus heart-specific deletion of Rb. Mol Cell Biol 2005;25:2486–2497
29. Haigis K, Sage J, Glickman J, Shafer S, Jacks T. The related retinoblastoma (pRb) and *p130* proteins cooperate to regulate homeostasis in the intestinal epithelium. J Biol Chem 2006;281:638–647
30. Harvey M, Vogel H, Lee EY, Bradley A, Donehower LA. Mice deficient in both *p53* and Rb develop tumors primarily of endocrine origin. Cancer Res 1995;55:1146–1151

31. Williams BO, Remington L, Albert DM, Mukai S, Bronson RT, Jacks T. Cooperative tumorigenic effects of germline mutations in Rb and *p53*. Nat Genet 1994;7:480–484
32. Vooijs M, van der Valk M, te Riele H, Berns A. Flp-mediated tissue-specific inactivation of the retinoblastoma tumor suppressor gene in the mouse. Oncogene 1998;17:1–12
33. Gannon M, Shiota C, Postic C, Wright CV, Magnuson M. Analysis of the Cre-mediated recombination driven by rat insulin promoter in embryonic and adult mouse pancreas. Genesis 2000;26:139–142
34. Nguyen KT, Tajmir P, Lin CH, Liadis N, Zhu XD, Eweida M, Tolasa-Karaman G, Cai F, Wang R, Kitamura T, Belsham DD, Wheeler MB, Suzuki A, Mak TW, Woo M. Essential role of Pten in body size determination and pancreatic β-cell homeostasis in vivo. Mol Cell Biol 2006;26:4511–4518
35. Iglesias A, Murga M, Laresgoiti U, Skoudy A, Bernales I, Fullaondo A, Moreno B, Lloreta J, Field SJ, Real FX, Zubiaga AM. Diabetes and exocrine pancreatic insufficiency in E2F1/E2F2 double-mutant mice. J Clin Invest 2004;113:1398–1407
36. Li FX, Zhu JW, Tessem JS, Beilke J, Varella-Garcia M, Jensen J, Hogan CJ, DeGregori J. The development of diabetes in E2f1/E2f2 mutant mice reveals important roles for bone marrow-derived cells in preventing islet cell loss. Proc Natl Acad Sci U S A 2003;100:12935–12940